Journal of Biomolecular Structure & Dynamics, ISSN 0739-1102
Volume 24, Issue Number 1, (2006)

Structural Differences Between Wild-type and Fish Eye Disease Mutant of Lecithin:cholesterol Acyltransferase

http://www.jbsdonline.com

Yana Reshetnyak[2,*]
Kissaou T. Tchedre[1]
Maya P. Nair[1]
P. Haydn Pritchard[3]
Andras G. Lacko[1,*]

[1]Department of Molecular Biology
and Immunology
University of North Texas Health Science Center
3500 Camp Bowie Blvd.
Fort Worth, Texas 76107, USA
[2]Department of Physics
University of Rhode Island
2 Lippitt Rd.
Kingston, Rhode Island 02881, USA
[3]Atherosclerosis Specialty Laboratory
Department of Pathology
and Laboratory Medicine
St. Paul's Hospital and
University of British Columbia
Vancouver, British Columbia
V6Z 1Y6, Canada

Abstract

Fluorescence spectroscopy has been used to investigate the conformational changes that occur upon binding of wild type (WT) and mutant (Thr123Ile) lecithin:cholesterol acyltransferase (LCAT) to the potential substrates (dioleoyl–phosphatidyl choline [DOPC] and high density lipoprotein [HDL]). For a detailed analysis of structural differences between WT and mutant LCAT, we performed decompositional analysis of a set of tryptophan fluorescence spectra, measured at increasing concentrations of external quenchers (acrylamide and KI). The data obtained show that Thr123Ile mutation in LCAT leads to a conformation that is likely to be more rigid (less mobile/flexible) than that of the WT protein with a redistribution of charged residues around exposed tryptophan fluorophores. We propose that the redistribution of charged residues in mutant LCAT may be a major factor responsible for the dramatically reduced activity of the enzyme with HDL and reconstituted high density lipoprotein (rHDL).

Introduction

Lecithin:cholesterol acyltransferase (LCAT EC2.3.1.43) is a key enzyme in cholesterol transport, controlling the flow of cholesterol from peripheral tissues to the liver (1, 2). LCAT catalyzes the esterification of plasma cholesterol, a rate limiting step in reverse cholesterol transport while interacting with high density lipoprotein (HDL) surfaces. Studies on the molecular structure of LCAT and its mutants have so far been hampered by the limited availability of highly purified enzyme preparations that yield diffraction quality crystals (2). The mutant form of LCAT ($LCAT_{Thr123Ile}$) was first described in a patient with fish eye disease and demonstrated the selective loss of alpha-LCAT activity (3), and subsequently studied in a number of laboratories (4-8).

One of the tryptophan residues (Trp61) has been proposed to function as a component of the interfacial recognition domain of LCAT (9, 10). Therefore, we applied the tryptophan fluorescence spectroscopy to investigate the structural properties of WT and mutant ($LCAT_{Thr123Ile}$) forms of LCAT and the conformational changes that occur upon their binding to potential substrates: (dioleoyl-phosphatidyl choline) DOPC, DOPC/cholesterol, and rHDL. We have employed the analysis of the decomposition of set of tryptophan fluorescence spectra, measured at various concentrations of external quenchers (acrylamide and KI) (11). The results of our analysis allowed us to identify structural differences between the WT and the mutant ($LCAT_{Thr123Ile}$) forms of LCAT.

Materials and Methods

Purification of Recombinant Human LCAT

Recombinant LCAT, secreting human lung cells, was obtained as described previously (14) in expanded to three layered flasks (Nunc Inc), and cultured in

[*]A. G. Lacko:
Phone: (817) 735-2132
Fax: (817) 735-2118
Email: alacko@hsc.unt.edu
Y. K. Reshetnyak:
Phone: (401) 874-5586
Fax: (401) 874-2380
Email: reshetnyak@mail.uri.edu

Dulbecco's modified Eagle's medium (DMEM-GIBCO/Invitrogen) with 2% fetal bovine serum (FBS) at 37 ºC in a 5% CO_2 atmosphere. The growth medium was subsequently removed and replaced with serum-free OPTI-MEM, once the cells were near confluence. The flasks were kept at 37 ºC for 30 minutes and then the OPTI-MEM was removed and replaced with fresh OPTI-MEM. The flasks were then incubated for 24 and 48 hrs at 37 ºC in a 5% CO_2 incubator to allow the secretion of the enzyme. The samples from the conditioned media were collected at 24 and 48 hrs and subjected to Phenyl-Sepharose chromatography as described previously (15). Approximately 800 ml culture medium containing the WT r-LCAT was loaded on a Phenyl-Sepharose column (2.5×18 cm), which had previously been equilibrated with 0.005 M PO_4, 0.3 M NaCl, pH 7.4. The column was washed with the same buffer until the absorbance at 280 nm decreased below 0.01. Subsequently, the purified LCAT was eluted with deionized water. The cell lines, stably transfected with the $LCAT_{Thr123Ile}$ mutant, were cultured the same way as the WT r-LCAT secreting human lung cells. The purified mutant enzyme ($LCAT_{Thr123Ile}$) was also prepared by Phenyl-sepharose chromatography as described above.

Preparation of DOPC, DOPC/Cholesterol and rHDL Complexes

The DOPC vesicles were prepared as follows. To 150 µl of 1 M DOPC (dissolved in chloroform), 0.1 ml of butylated hydroxy-toluene, and 1 ml of chloroform were added. The mixture was subsequently dried to a thin film in a water bath at 37 ºC, under an N_2 stream. The dry film then was redissolved in 0.5 ml absolute ethanol and injected into 30 ml of 0.01M Tris, 0.005M EDTA, 0.15 M NaCl, pH 7.4 (TEN buffer) with a 25 gauge needle, while stirring. After stirring for about 20 min, the volume of the DOPC emulsion was increased to 50 ml with TEN Buffer.

The preparation of the DOPC/cholesterol vesicles was essentially the same as that of the DOPC vesicles except that 119 µl of unesterified cholesterol (50 mg/ml) was added to 150 µl of 1 M DOPC (dissolved in chloroform).

Reconstituted HDL (rHDL) was prepared as follows: chloroform solutions of 1.8 mg of egg yolk phosphatidyl-choline (Sigma), 0.45 mg of unesterified cholesterol and 0.9 mg cholesteryl oleate were combined and the mixture was dried to a thin film in a water bath at 37 ºC, under an N_2 stream. Subsequently 5 ml of 10mM Tris, 0.1 M KCl, 1 mM EDTA pH 8.0 was added and the mixture was vortexed and sonicated for 60 min at 60 ºC. Apolipoprotein-AI ([Apo-AI], 10 mg) was added in 3 M Guanidine.HCl and the mixture was sonicated for an additional 30 minutes at 42 ºC. The HDL-sized particles were isolated by density gradient ultracentrifugation (16) and the preparation was dialyzed against PBS overnight and stored at 4 ºC.

Fluorescence and Light Scattering Measurements

Tryptophan fluorescence and light scattering measurements were carried out on a digital phase-modulation spectrofluorometer ISS K2 (ISS, Champagne, IL) at 25 ºC in a buffer solution containing 50 mM KCl, 10 mM Tris-HCl, pH 7.5 with LCAT concentrations varied from 1-4 µM. The excitation wavelength was 295 nm for the excitation of only tryptophan fluorophores in protein. The emission spectra were recorded from 314 to 400 nm with the spectral widths of excitation and emission slits set at 4 and 2 nm, respectively. However, for the decomposition analysis we used range of 320-380 nm to exclude the contribution of light scattering at short wavelengths and reduce errors of low intensities at long wavelengths. The polarizers in the excitation and emission paths were set at "magic" angle (54.7º from the vertical orientation) and vertically (0º), respectively, in order to reduce Wood's anomalies from reflecting holographic grating (17). The emission spectrum of an aqueous solution of L-tryptophan was used as a standard for

the correction of protein spectra for the instrument spectral sensitivity (18). The intensities of the corrected spectra are proportional to the number of photons emitted per unit wavelength interval. The light scattering (*S*) was measured at 400 nm wavelength settings of the excitation and emission monochromators. The anisotropy (*r*) measurements were performed at excitation and emission wavelength set up at 295 and 340 nm, respectively.

Decomposition of Tryptophan Fluorescence Spectra

For the decomposition analysis, the tryptophan fluorescence spectra of WT and mutant proteins excited at 295 nm were obtained in the presence of increasing concentrations of the external quenchers. We used acrylamide and potassium iodide at concentration of 0, 0.073, 0.14, 0.2, 0.26, 0.32, 0.4 M as external quenchers of tryptophan fluorescence (19-21). When ionic quencher (I^-) was used the total ionic strength was kept constant (0.4 M) by additions of KCl. In experiments with acrylamide the intensities in fluorescence spectra were corrected for the screening inner filter effect of this quencher at the excitation wavelength of 295 nm. The temperature was kept constant at 25 ºC. Decomposition of the protein fluorescence spectra at different concentration of quenchers was performed according to Burstein *et al*., 2000 (11). Briefly, the shape of each spectral component of protein fluorescence spectra on the frequency (wavenumber) scale was approximated by uni-parametric log-normal function (first, the fluorescence spectra were converted to the frequency scale from the wavelength scale $F_\nu = F_\lambda \cdot \lambda^2$). The intensities for the components were calculated from the set of linear equations. The shape and position of spectral components remain unchanged at fluorescence quenching with water-soluble quenchers and the change in intensity of individual components with quenching was checked to obey the Stern-Volmer law. The resolution into components was performed using SIMS (SImple fitting with Mean-Square criterion) and PHREQ (Phase-plot-based REsolution using Qenchers) algorithms. The spectra were independently fitted by one, two, or three components. Typical experimental noise of fluorescence spectra, which is about 0.5-1.5%, does not permit a sufficiently reliable decomposition for more than three spectral components. The criterion of attaining the best solution (a sufficient number of components) was the minimal root-mean-square differences (residuals) between theoretical and experimental spectra. For each *i*-th component, the program output data contained the values of spectral maximum position $\lambda_m(i)$, the per-cent contribution of the component into the area under total spectrum $F(i)$, Stern-Volmer quenching constant $K_{SV}(i)$, and its ratio to the K_{SV} value for free aqueous tryptophan emission quenching with the same quencher, $K_{rel}(i)$. The Stern-Volmer constants $K_{SV}(i)$ were calculated as slopes of the linear plots in coordinates $(A_o/A_c - 1)$ vs. quencher concentration, where A_o and A_c are areas under emission component spectra measured, respectively, in the absence (A_o) and in the presence of quencher in the concentration c (A_c). In order to calculate K_{rel} value, the K_{SV} value for dynamic quenching of free aqueous tryptophan emission with acrylamide and iodide were taken to be 16.8 M^{-1} and 14.6 M^{-1}, respectively.

Binding of Enzyme with DOPC and rHDL

The binding affinity of WT and mutant LCAT to DOPC and DOPC/Cholesterol complex was monitored by the increasing of quantum yield of fluorescence. Five samples of DOPC and DOPC/Cholesterol emulsions were prepared representing PC/LCAT molar ratios of 0, 20, 80, 120, 200. For the rHDL affinity studies, the difference spectra were obtained by subtracting the fluorescence of LCAT incubated with rHDL for 10 min from the sum of two individual spectra (LCAT plus rHDL) measured separately. The concentration of the protein was kept constant (1 μM). The concentration of rHDL in solution, based on the cholesterol content of HDL (HDL-C) was increased from 0 to 10 μM (in the increments of 0.1, 0.5, 1, 5, 10 μM).

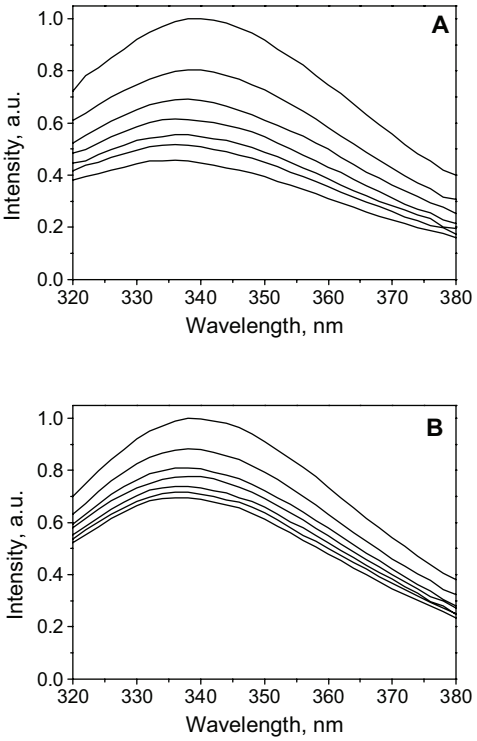

Figure 1: Corrected tryptophan fluorescence spectra of WT LCAT (4 μM) measured at increasing concentrations (0, 0.073, 0.14, 0.2, 0.26, 0.32, 0.4 M) of quenchers acrylamide (**A**) and KI (**B**). The emission spectrum of an aqueous solution of L-tryptophan was used as a standard for the correction of protein spectra for the instrument spectral sensitivity. The excitation wavelength was 295 nm, T = 25 ºC, the polarizers in the excitation and emission paths were set at 54.7º and 0º, respectively. In experiments with acrylamide the intensities in fluorescence spectra were corrected for the screening inner filter effect of this quencher at the excitation wavelength of 295 nm. When ionic quencher (I^-) was used the total ionic strength was kept constant (0.4 M) by additions of KCl.

Results

Decomposition Analysis of Tryptophan Fluorescence Spectra of WT and Mutant LCAT

The fluorescence parameters for both proteins are summarized in Table I. Both enzymes emitted at the intermediate wavelength of 336 nm with the quantum yield of the mutant protein being 88% of that of the WT enzyme. The anisotropy value of the mutant protein was higher than that of the WT, while the light scattering values for both WT and mutant LCAT were very similar.

Table I

Fluorescence parameters of WT and mutant LCAT. All measurements were performed several times and standard deviations are presented.

Experimental parameters	LCAT-WT	LCAT-mutant
Maximum position of total fluorescence spectrum, nm (λ_m)	336.8 ± 0.5	336.0 ± 0.5
Area under the spectrum, % (A)	100	88
Anisotropy (r)	0.18 ± 0.01	0.22 ± 0.01
Light scattering, a.u. (S)	670 ± 20	692 ± 20

To better define structural differences between two forms of the enzyme, we performed the decomposition of tryptophan fluorescence spectra into spectral component (11). Both WT and mutant LCAT exhibited non-homogeneous emission profiles considering that the fluorescence spectra were wider than those of known proteins with homogeneous fluorescence with a maximum at 336 nm (12, 18, 22). Heterogeneity of the emission spectra is attributed to the presence of more than one type of emitting tryptophan residue representing distinct structural classes within the protein molecule (13). In order to resolve the spectral heterogeneity and examine the contributions of individual tryptophan residues (or clusters of tryptophan residues), we used the decomposition analyses of the fluorescence spectra of WT and mutant LCAT. The spectral components obtained in a result of decomposition analyses of more than 150 proteins showed excellent correlation with the structural properties of tryptophan fluorophores in proteins (12-13). Recently additional supportive evidence was obtained of the predictive value of decomposition algorithms *via* analysis of the correlation with the experimental spectra of single-tryptophan-containing mutants of membrane protein OEP16 (23).

The rate of fluorescence quenching by acrylamide and KI was different (Figure 1); however, the decomposition analyses for both quenchers gave the same results (first columns, Table II), attesting the validity of the decomposition analysis. The data summarized in Table II [columns: $\lambda_m(i)$ and $F(i)$] represent the spectral components and their contributions to the total fluorescence spectra of WT and mutant LCAT at 0 M concentration of quenchers. For both WT and mutant proteins, three spectral components were identified. The first component has a maximum at 310.8 nm while the other two components have longer-wavelength maxima at ~ 338 and 343-

Table II

The results of decomposition of tryptophan fluorescence spectra of WT and mutant LCAT measured at various concentrations of acrylamide and KI (the details of experiments are described in text and legend to Figure 1): number of spectral components (i), maximum position (λ_m(i), nm) and contribution (F(i), %) of spectral components in total fluorescence spectrum measured at 0 M concentration of acrylamide and KI, absolute (K_{SV}^{Ac}(i), M^{-1}, K_{SV}^{KI}(i), M^{-1}) and relative (K_{rel}^{Ac}(i), %, K_{rel}^{KI}(i), %, see explanation in the text) Stern-Volmer quenching constants for acrylamide and KI. All measurements were performed several times and standard deviations for each spectral parameter are indicated.

Sample	i	λ_m(i), nm	F(i), %	K_{SV}^{Ac}(i), M^{-1}	K_{rel}^{Ac}(i), %	K_{SV}^{KI}(i), M^{-1}	K_{rel}^{KI}(i), %
LCAT-WT	1	310.8 ± 2.3	15.2 ± 2.4	0.70 ± 0.33	4.2 ± 2.0	0.72 ± 0.20	4.9 ± 1.4
	2	338.3 ± 1.5	35.4 ± 1.6	1.94 ± 0.59	11.5 ± 3.5	0.02 ± 0.26	0.0 ± 1.8
	3	343.6 ± 0.8	49.4 ± 1.9	6.79 ± 1.6	40.4 ± 9.5	6.95 ± 1.14	47.6 ± 7.8
LCAT-mutant	1	310.8 ± 1.8	16.5 ± 1.1	1.20 ± 0.35	7.1 ± 2.1	0.65 ± 0.41	4.5 ± 2.8
	2	338.9 ± 1.0	30.9 ± 4.9	1.27 ± 0.44	7.6 ± 2.6	1.46 ± 0.96	10.0 ± 6.6
	3	344.7 ± 0.5	40.6 ± 3.8	7.05 ± 1.31	42.0 ± 7.8	4.13 ± 1.07	28.3 ± 7.3

344 nm, respectively. The absolute (K_{sv}) and relative (K_{rel}) Stern-Volmer constants for each spectral components for acrylamide and iodide quenchers were calculated. The relative Stern-Volmer constants were derived from K_{sv}, based on the assumption that 100% corresponds to the quenching of the fluorescence of free tryptophan in solution by acrylamide and KI, which are 16.8 M^{-1} and 14.6 M^{-1}, respectively. Although the maxima of the respective spectral components of the WT and mutant proteins were the same, the contributions of the spectral components to the total fluorescence and Stern-Volmer quenching constants were different.

Binding of WT and Mutant LCAT to DOPC, DOPC/Cholesterol, and HDL

The binding of WT and mutant LCAT to DOPC and HDL was also studied using fluorescence spectroscopy. As DOPC have no fluorescence at 300-400 nm, the binding of DOPC and DOPC/Cholesterol to LCAT was monitored by the increase in the quantum yield of LCAT fluorescence. The data in Figure 2 show the changes of the area under the spectra (Figure 2A) and the emission wavelength of fluorescence spectra (Figure 2B) for the WT and mutant LCAT proteins upon exposure to DOPC and DOPC/Cholesterol. The X axis represents the excess of PC concentration over protein concentration: R = [concentration of PC in DOPC or DOPC/Cholesterol] / [concentration of protein]. The fluorescence of the WT and mutant LCAT are altered in response to the binding of the respective proteins to DOPC and DOPC/Cholesterol, as the quantum yield increased due to increased exposure to the lipid complexes, in addition to the spectral shift to 332 nm. In Figure 2B, the changes in the maximum position of fluorescence spectra of WT are shown during interaction with DOPC. Essentially identical data were obtained for the mutant form of LCAT and both forms of the enzyme in the presence of DOPC/Cholesterol. The enhancement of fluorescence and the blue-wavelength shift in the maximum position of spectra indicated that the exposed tryptophan residues are likely to be located in the phospholipid binding domain of LCAT, based on the altered fluorescence parameters in the presence of DOPC.

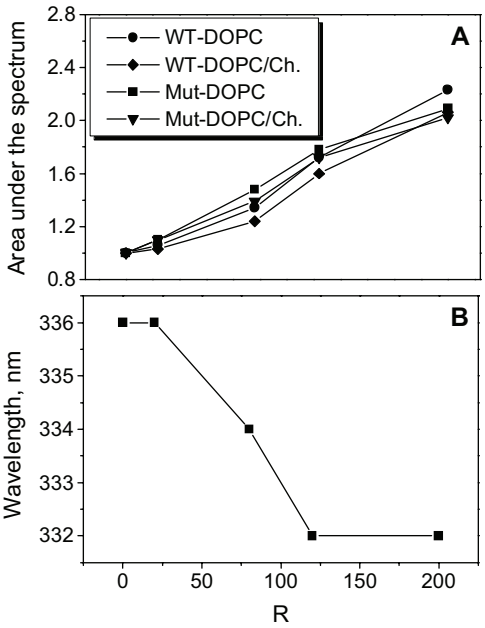

Figure 2: The titration of LCAT with DOPC and DOPC/Cholesterol. The dependence of area under the corrected tryptophan fluorescence spectra (**A**) and emission wavelength (**B**) of WT and mutant LCAT measured in the presence of different concentration of DOPC and DOPC/Cholesterol. The X axis represents the excess of PC concentration over protein concentration: R = [concentration of PC in DOPC or DOPC/Cholesterol] / [concentration of protein].

Figure 3 shows the fluorescence spectra of 1 μM LCAT with 10 μM HDL (monitored after a 10 min incubation of the respective LCAT samples with HDL). The controls for these studies consisted of the sum of each spectra of the same amount of LCAT and HDL, measured separately. The difference spectrum is inserted in

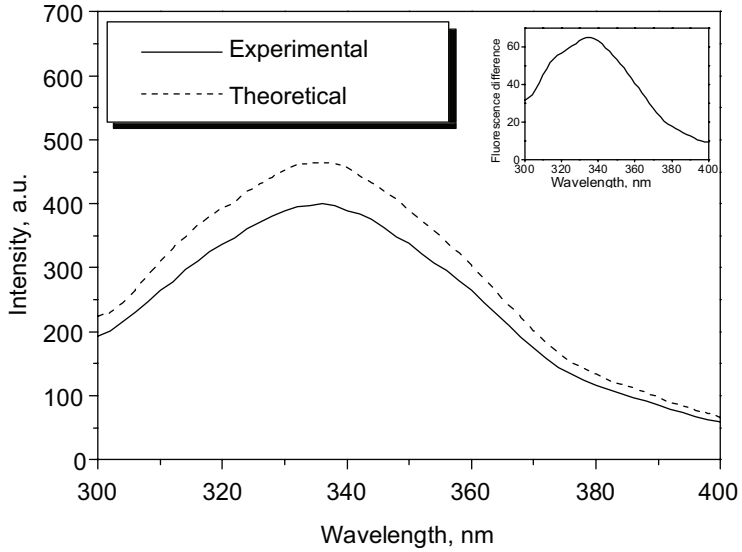

Figure 3: Comparison of experimental and theoretical tryptophan fluorescence spectra of LCAT and HDL. The solid line represents fluorescence spectrum of 1 μM of WT protein incubated with 10 μM of HDL during 10 min. The dashed line represents the sum of fluorescence spectra of 1 μM WT protein and 10 μM HDL measured separately. The difference spectrum between theoretical and experimental emission spectra is plotted in the inset.

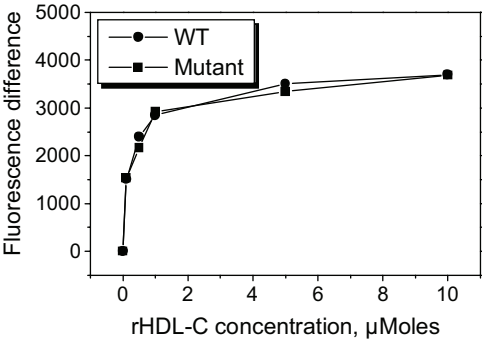

Figure 4: The titration of LCAT with rHDL. The dependence of the area under the difference fluorescence spectra of WT and mutant LCAT incubated with rHDL and the sum of protein and rHDL spectra measured separately from the concentration of rHDL.

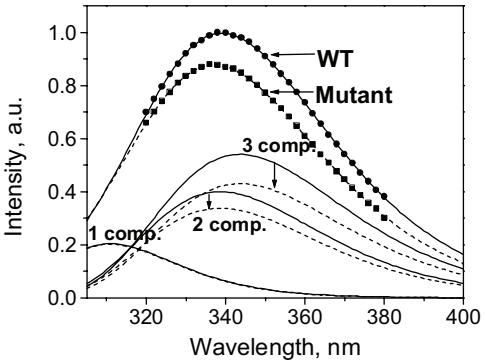

Figure 5: Decomposition of corrected tryptophan fluorescence spectra of WT (solid lines) and mutant (dashed lines) LCAT. The fluorescence maximum positions and changes in relative contributions of components are given in Table II and III, respectively. The fluorescence was excited at 295 nm.

Figure 3. We investigated the binding of WT and mutant forms of LCAT to HDL by analyzing the difference spectra obtained from the incubation studies (Figure 4).

Discussion

We have investigated the structural differences of a recombinant wild type enzyme and mutant LCAT (Thr123Ile), stably expressed in baby hamster kidney cells and conformational changes, which occur in proteins upon binding with DOPC, DOPC/cholesterol, and HDL. Fluorescence spectroscopy was used in this study to investigate the structure and dynamics (24) of the two forms of LCAT. Several spectral parameters, including maximum position and shape of tryptophan fluorescence spectra, quantum yield, anisotropy, light scattering and degree of quenching of tryptophan fluorescence by acrylamide, and KI were analyzed for WT and mutant LCAT. In addition, we applied the analysis of the decomposition of tryptophan fluorescence spectra into spectral components to identify distinct emitting and structural classes of tryptophan residues in both proteins (11-13).

The changes of spectral characteristics of mutant LCAT in comparison with WT LACT are summarized in Table III. We detected no changes in maximum position of fluorescence spectra, but some decrease (12%) of the intensity of fluorescence signals was found, in good agreement with previous studies (6). In addition, we identified small (10%) but significant changes of anisotropy values. The anisotropy value of 0.4, which corresponds to the maximal theoretically possible value for the rigid dipoles (24), was taken as 100%. We did not detect any changes in light scattering, which indicates no significant changes in shape of mutant protein. We performed the decomposition analysis of tryptophan fluorescence spectra of both proteins and identified three spectral components, corresponding to three classes of tryptophan residues each with distinct structural interactions with their respective environments for both WT and mutant LCAT. However, while the maximum position of the spectral components remain unchanged, the contributions of the second and third components decreased (Figure 5), indicating that the conformational changes may be accompanied by enhancing of the quenching of tryptophan emission by neighboring residues in the mutant protein.

Table III

The difference of the spectral properties between mutant and WT LCAT: shift of the total fluorescence spectrum in nm ($\Delta\lambda_m$), the changes in total quantum yield (ΔA, %,), anisotropy (Δr,%) and light scattering (ΔS, %) values; shift of maximum positions of spectral components ($\Delta\lambda_m$(i), nm), the changes of the contributions of spectral components in total fluorescence (ΔF(i), %) and relative Stern-Volmers constants for acrylamide (ΔK_{rel}^{Ac}(i), %) and KI (ΔK_{rel}^{Ac}(i), %).

$\Delta\lambda_m$, nm	ΔA, %	Δr,%	ΔS,%	i	$\Delta\lambda_m$(i), nm	ΔF(i), %	ΔK_{rel}^{Ac}(i), %	ΔK_{rel}^{KI}(i), %
				1	0	-0.7	2.9	-0.4
-0.8	-12	10	3.3	2	0.6	-8.2	3.9	10.0
				3	1.1	-13.7	1.6	-19.3

The first class of tryptophan residues is considered buried in the interior of protein molecules where the tryptophan fluorophores are surrounded by a rigid, nonmobile environment. It is expected that all neighboring atoms of the tryptophan residues emitting at short wavelengths are involved in the stabilization of the secondary structure of both proteins (13). These types of tryptophan residues are characterized by an extreme blue-shift resulting in an emission maximum of ~ 310 nm and practically zero Stern-Volmer constant. We did not observe any changes of spectral properties (maximum position, contribution in total fluorescence, Stern-Volmer constants) of tryptophan residues corresponding to the first component in the mutant form of LCAT.

The second spectral component (338-340 nm) represents the class of tryptophan fluorophores more exposed to a hydrophilic environment and being primarily in contact with structured-water molecules. The environment of these tryptophan

residues is more flexible, consisting of mobile protein atoms, in addition to structured-water molecules (13). We found that the contribution of the second spectral component decreased 8.2% in mutant LCAT in comparison with the WT protein. In addition, we found a small (3.9%) and significant (10%) increases in the degree of fluorescence quenching by neutral molecule (acrylamide) and ionic quencher (I^-), respectively. The Stern-Volmer constant (K_{SV}^{KI}) for the second spectral component of WT protein is around zero (see Table II). Such extremely low value of quenching for the fluorophores emitting at 338 nm could be explained by the presence of negatively charged residues (Glu or Asp), which repulse iodide ion, around fluorophores. Our data might indicate that Thr123Ile mutation leads to the changes in charge distribution (decreasing of negative charges) around tryptophan residues contributing to the second component that leads to the enhancement of fluorescence quenching by KI.

The third class of tryptophan residues with a fluorescence maximum at 344-345 nm is exposed to a highly mobile environment, including free water molecules. The maximum position of the exposed fluorophores in native proteins could vary from 344 to 349 nm (13). The decomposition analysis showed that while the respective positions of the spectral components were the same; their contributions to the total fluorescence of the WT vs. the mutant protein were substantially different. Accordingly, the contributions of the exposed tryptophan residues were lower (13.7%) in the mutant LCAT. Again we did not observe any changes in the degree of acrylamide quenching and no changes in the maximum position of spectral component, while we found significant decrease (19.3%) in iodide quenching, which might indicate the changes in charge distribution (increase positive charges around tryptophan fluorophores) of mutant LCAT.

Summarizing all monitored changes of spectral properties, we concluded that Thr123Ile mutation in LCAT might lead to the conformational changes that result in i) more rigid, less mobile/flexible conformation of the whole protein with ii) new redistribution of charged residues around exposed tryptophan fluorophores: decrease and increase of negative charges around tryptophan fluorophores emitting at 338-340 nm and 343-344 nm, respectively.

Regardless of evident structural diversity between WT and mutant ($LCAT_{Thr123Ile}$) LCAT we did not observe any differences in binding of these proteins to DOPC, DOPC/Cholesterol, or HDL. Previously, it was proposed that the defect in $LCAT_{Thr123Ile}$ mutant is not in the initial, interfacial binding step to lipoproteins but rather in subsequent steps of the reaction cycle (7). The analysis of equilibrium binding constants, measured directly with surface plasmon resonance, indicated that the affinity of the mutant for rHDL was much higher than its activity (7). On the other hand, the heat changes of mutant LCAT measured by isothermal titration calorimetry (ITC) were very small in comparison with WT LCAT (7). Our conclusion about redistribution of charged residues in mutant LCAT is consistent with the monitored differences in heat changes of WT and mutant LCAT binding with rHDL and it could be interpreted that the binding of mutant protein with rHDL is driven by hydrophobic interactions. The mutant $LCAT_{Thr123Ile}$ had markedly depressed (on 90%) reactivity with reconstituted HDL, but it retained activity with low density lipoprotein (25, 26). Also, it was demonstrated the direct protein-protein interaction between LCAT and apo-AI (27, 28) and the significant role of charged residues in modulation of the catalytic efficiency of the LCAT (29-31). We propose that the redistribution of charged residues in mutant LCAT might be considered as a major factor of the dramatically reduced activity of LCAT with HDL and rHDL (containing apo-AI). However, the charge redistribution does not affect the binding affinity of the enzyme for DOPC and DOPC/cholesterol.

Acknowledgement

This work was supported by a grant (# 0150730Y) from the American Heart Association-Texas Affiliate.

References and Footnotes

1. S. Santamarina-Fojo, G. Lambert, J. M. Hoe, and H. B. Brewer. *Curr. Opin. Lipidol. 11*, 267-275 (2000).
2. A. Jonas. *Biochim. Biophys. Acta. 1084*, 205-220 (1991).
3. H. Funke, A. von Eckardstein, P. H. Pritchard, J. J. Albers, J. J. Kastelein, C. Droste, and G. Assmann. *Proc. Natl. Acad. Sci. USA 88*, 4855-4859 (1991).
4. K. S. Chong, M. Jahani, S. Hara, and A. G. Lacko. *Can. J. Biochem. Cell Biol. 61*, 875-881 (1983).
5. K. O. J. S. Hill, X. Wang, and P. H. Pritchard. *J. Lipid Res. 34*, 81-88 (1993).
6. S. Adimoolam, L. Jin, E. Grabbe, J. J. Shieh, and A. Jonas. *J. Biol. Chem. 273*, 32561-32567 (1998).
7. L. Jin, J. J. Shieh, E. Grabbe, S. Adimoolam, D. Durbin, and A. Jonas. *Biochemistry 38*, 15659-15665 (1999).
8. K. R. Murray, M. P. Nair, A. F. Ayyobi, J. S. Hill, P. H. Pritchard, and A. G. Lacko. *Arch. Biochem. Biophys. 385*, 267-275 (2001).
9. F. Peelman *et al. Protein Eng. 12*, 71-78 (1999).
10. K. Wang and P. V. Subbaiah. *Biochem J. 365*, 649-657 (2002).
11. E. A. Burstein, S. M. Abornev, and Y. K. Reshetnyak. *Biophys. J. 81*, 1699-1709 (2001).
12. Y. K. Reshetnyak and E. A. Burstein. *Biophys. J. 81*, 1710-1734 (2001).
13. Y. K. Reshetnyak, Y. Koshevnik, and E. A. Burstein. *Biophys. J. 81*, 1735-1758 (2001).
14. J. S. Hill, K. O. X. Wang, S. Paranjape, D. Dimitrijevich, A. G. Lacko, and P. H. Pritchard. *J. Lipid Res. 34*, 1245-1251 (1993).
15. M. P. Nair, B. J. Kudchodkar, P. H. Pritchard, and A. G. Lacko. *Protein Expr. Purif. 10*, 38-41 (1997).
16. A. H. Terpstra, C. J. Woodward, and F. J. Sanchez-Muniz. *Anal Biochem. 111*, 149-157 (1981).
17. D. Kessel. *Photochem Photobiol. 54*, 481-483 (1991).
18. E. A. Burstein and V. I. Emelyanenko. *Photochem. Photobiol. 64*, 316-320 (1996).
19. M. R Eftink. *Meth. Biochem. Analysis 35*, 127-205 (1991).
20. S. S. Lehrer and P. C. Leavis. *Methods Enzymol. 49*, 222-236 (1978).
21. E. A. Burstein. *Biophysics* (Moscow) *13*, 433-442 (1968).
22. E. A. Burstein, N. S. Vedenkina, and M. N. Ivkova. *Photochem. Photobiol. 18*, 263-279 (1973).
23. D. Linke, J. Frank, M. S. Pope, J. Soll, I. Ilkavets, P. Fromme, E. A. Burstein, Y. K. Reshetnyak, and V. I. Emelyanenko. *Biophys.J. 86*, 1479-1487 (2004).
24. J. R. Lakowicz. *Principles of Fluorescence Spectroscopy*, 2nd Edition. Kluwer Academic/Plenum Publishers, New York (1999).
25. L. Holmquist and L. A. Carlson. *Acta. Med. Scand. 222*, 23-26 (1987).
26. K. O. J. S. Hill, X. Wang, and P. H. Pritchard. *J. Lipid Res. 34*, 81-88 (1993).
27. G. Knipping, A. Hermetterand, and M. R. Hubmann. *Int. J. Biochem. 25*, 505-511 (1993).
28. F. Peelman, J. L. Verschelde, C. Ampe, C. Labeur, J. Tavernier, J. Vandekerckhove, and M. Rosseneu. *J. Lipid Res. 40*, 59-69 (1999).
29. F. Peelman, B. Vanloo, J. L. Verschelde, C. Labeur, H. Caster, J. Taveirne, A. V. B. N. Duverger, J. Vandekerckhove, J. Tavernier, and M. Rosseneu. *J. Lipid Res. 42*, 471-479 (2001).
30. Y. Zhao, J. Wang, A. K. Gebre, J. W. Chisholm, and J. S. Parks. *Biochemistry 42*, 13941-13949 (2003).
31. E. T. Alexander, S. Bhat, M. J. Thomas, R. B. Weinberg, V. R. Cook, M. S. Bharadwaj, and M. Sorci-Thomas. *Biochemistry 44*, 5409-5419 (2005).

Date Received: January 13, 2006

Communicated by the Editor Valery Ivanov